The Egyptian Journal of Radiology and Nuclear Medicine (2014) **45**, 1115–1125

Egyptian Society of Radiology and Nuclear Medicine

The Egyptian Journal of Radiology and Nuclear Medicine

www.elsevier.com/locate/ejrnm
www.sciencedirect.com

ORIGINAL ARTICLE

Diagnostic accuracy of diffusion weighted MRI in cervical lymphadenopathy cases correlated with pathology results

Noha Abd ElShafy ElSaid *, Omnia Mokhtar Mohamed Nada, Yomna Sameh Habib, Ahmed Reda Semeisem, Nagat Mansour Khalifa

National Cancer Institute, Cairo University, Egypt

Received 5 February 2014; accepted 26 June 2014
Available online 3 August 2014

KEYWORDS

MRI;
Diffusion weighted MRI;
Cervical lymphadenopathy

Abstract *Introduction:* Diffusion weighted magnetic resonance imaging (DW MRI) is an imaging technique showing molecular diffusion. Cell size, density and integrity influence the signal intensity seen on diffusion-weighted images. This technique is a helpful complementary tool to distinguish tumoral from non tumoral tissue.

The aim of this prospective study is to define the diagnostic accuracy of DWI to differentiate benign from malignant cervical lymph nodes.

Patients and methods: Twenty six patients who presented with 32 nodes were included in this study, 9 males (35.6%) and 17 females (65.4%). Their age ranged from: 6 to 76 years, mean age 45 ± 18.8 years referred to the radiology department of NCI, complaining of neck swelling, ultrasound showed cervical nodes.

Results: According to histopathological analysis we divided the examined lymph nodes (n = 32) into 2 categories: malignant lymph nodes 75% (n = 24) benign lymph nodes 25% (n = 8). DWI and ADC (apparent diffusion coefficient) values revealed 27 malignant lesions (84%), 5 benign (16%). The accuracy of the DWMRI was 89%. A significant difference between benign and malignant cervical nodes on DWI and on ADC maps is reported.

The results obtained were 24 true positive, 3 false positive, 5 true negative. No false negative cases were identified, yielding a sensitivity of 100%, specificity of 62.5%, NPV = 100% and PPV = 89%. The difference between the mean ADC values between benign and malignant lesions was statistically significant (P < 0.0001).

Conclusion: MR diffusion imaging could be an important supportive tool in differentiation between benign and malignant lymph nodes, can to a lesser extent differentiate between the types

* Corresponding author.
E-mail address: nohashafi@yahoo.com (Noha Abd ElShafy ElSaid).
Peer review under responsibility of Egyptian Society of Radiology and Nuclear Medicine.

http://dx.doi.org/10.1016/j.ejrnm.2014.06.012

of malignant lymphadenopathy and can be used as an indicator for improvement and recurrence post chemo and radiotherapy.

1. Introduction

Lymphadenopathy is an abnormal increase in size and/or altered consistency of the lymph nodes. The condition is generally not a disease by itself, rather, it may be a symptom of one of many possible underlying problems and serves as an excellent clue to them. It could be due to infections, autoimmune disorders or malignancies (metastatic or lymphomas) (1).

Nodal metastases are an adverse prognostic factor in patients with head and neck squamous cell carcinoma (HNSCC) not only for the planning of appropriate treatment but also for monitoring the treatment response. Imaging is used in addition to clinical evaluation to improve the detection of nodal metastases (2).

In case of lymphoma, DWI could be used not only in a pre-treatment phase, but also after therapy to detect recurrent disease or as sign of improvement (3).

Small lymph nodes with a maximum short axial diameter below 10 mm are more challenging for radiologists, because the mere use of this size criterion will result in misclassification of malignant lymph nodes as normal on MRI evaluation (2).

Diffusion-weighted magnetic resonance imaging (DWMRI) is an imaging technique showing molecular diffusion. Cell size, density and integrity influence the signal intensity seen on diffusion-weighted images. This technique is a helpful complementary tool to distinguish tumoral from non-tumoral tissue, and has several interesting applications in the evaluation of head and neck cancer especially in head and neck lymphadenopathy (4).

Although diffusion-weighted MRI (DWI) has been used for some time for brain evaluation, extra cranial applications of diffusion-weighted (DW) magnetic resonance (MR) imaging are gaining importance. DWI is able to characterize tissue based on differences in water mobility (5).

Hypercellular tissue, such as occurring within malignant tumors, will show low ADC values. Non-tumoral tissue changes such as edema, inflammation, fibrosis, and necrosis are expected to show low cellularity, in strong contrast with viable tumor. This results in a high ADC. An inverse correlation between the ADC value and tumor cellularity in experimental models has been shown, and this has been clinically validated (3).

Differentiation of treatment-induced tissue changes, especially after chemo and/or radiotherapy, and persistent or recurrent cancer, is another area in which DWI may be very helpful. As DWI allows differentiation between inflammatory and neoplastic tissues, another possible application could be the monitoring of tumor response during radiotherapy: this could have prognostic importance and possibly influence the management of the patient (2).

The aim of this prospective study is to define the diagnostic accuracy of DWI to differentiate benign from malignant cervical lymph nodes.

2. Patients and methods

2.1. Patients

Our prospective study cohort included 26 patients with palpable 32 neck nodes, 9 males (35.6%) and 17 females (65.4%). Their age ranged from 6 to 76 years, mean age 45 ± 18.8 years.

All the patients were referred from the outpatient clinics to the radiology department in National cancer institute. Eleven patients presented with palpable cervical lymph nodes with unknown primary. They underwent neck US or CT before MRI examination. Ten patients with known head and neck cancer underwent MRI for staging and therapy planning. Five patients were coming for routine follow up post total thyroidectomy and radioactive iodine therapy.

Moreover we studied 1 patient with Hodgkin lymphoma after chemotherapeutic treatment. Follow up DWI was done in this case; comparison regarding the size of LN and ADC was performed. Biopsy was done in this case and revealed good therapeutic response.

- Inclusion criteria
  - Patients presenting with enlarged cervical lymph nodes as a first presentation or with known head and neck cancer.
- Exclusion criteria
  - Patient who has one or more of the absolute or relative MRI contraindications i.e. patient with one or more of the following:
    1. Electronically, magnetically and mechanically activated implants.
    2. Ferromagnetic or electronically operated active devices.
    3. Cardiac pacemakers.
    4. Metallic splinters in the eye.
    5. Ferromagnetic hemostatic clips in the central nervous system (CNS).
    6. Cochlear implants.
    7. Insulin pumps and nerve stimulators.
    8. Prosthetic heart valves (in high fields, if dehiscence is suspected).

2.1.1. Patients were subjected to the following

Full clinical assessment including recording of age, sex and clinical presentation.

Laboratory investigations [coagulation profile, renal function tests (blood urea and serum creatinine)].

MRI neck (pre- and post contrast study and diffusion-weighted imaging) results were compared to histopathology results in all patients.

US guided biopsies were done for the suspicious cervical lymph nodes in 22 patients in our study, only 4 patients underwent excisional biopsies after taking the patient's consent.

All MR examinations were performed with a 1.5-T whole-body system (Intera NT; Philips Medical Systems, Best, the Netherlands) with a 30 mT/m maximum gradient capability in NCI. A standard receive-only head and neck coil was used for both conventional imaging and diffusion-weighted MR imaging to include nodes from the base of the skull to the suprasternal notch.

In all patients, the protocol included:

- Fast spin echo (FSE) T2-weighted images (TR 2500–4500 ms, TE 80 ms, slice-thickness: 5 mm) in axial plane; with no intersection gap; number of signals acquired 4, Voxel size: RL 0.9, AP 1.1.
- Fast spin echo (FSE) T2-weighted images (TR 3850 ms, TE 75 ms, slice-thickness: 5 mm), in coronal plane.
- Fast spin echo (FSE) T1-weighted images, with and without fat suppression (TR 400–650 ms, TE 14 ms, slice-thickness: 5 mm) in axial plane; with no intersection gap; number of signals acquired 4, Voxel size: RL 0.9, AP 1.1.
- Fast spin echo (FSE) T1-weighted images, with fat suppression SPAIR: (Spectral Attenuated Inversion Recovery) after contrast medium administration of 0.1 mmol/kg of Omniscan (gadodiamide), GE Healthcare); in axial and coronal planes.

Diffusion-weighted MR imaging was performed before the contrast-enhanced T1-weighted MR imaging sequence using a spin-echo single shot T2 weighted echo-planar imaging sequence with the following parameters:

2000/75; section thickness, 4 mm, with no gap; field of view, 230 mm; acquisition matrix, 112×112; reconstruction matrix, 256×256; pixel resolution of $2.0 \times 2.0 \times 4.0$ mm.

Diffusion gradient encoding in three (x, y, z) orthogonal directions.

b values were of 0, 1000 s/mm^2. At each *b* value, x, y, and z single-direction DW images and a baseline image (*b* _ 0 s/mm^2) were acquired; combined ([x _ y _ z]/3). DW imaging was performed and calculated automatically by the MR instrument. 11 fat-suppressed diffusion-weighted MR images in the head and neck were acquired in the transverse plane.

Parallel imaging with generalized auto-calibrating partially parallel acquisition (GRAPPA) with an acceleration factor of two was applied to improve image quality.

All DW imaging data were transferred to a computer workstation for determination of the signal intensity and ADC (apparent diffusion coefficient). The ADC map was automatically reconstructed by a standard software imager in the main console. The ADC was measured by manually placing regions of interest on the ADC map. The ADC was measured twice and the two measurements were averaged. To ensure that the same areas were measured, regions of interest were copied and pasted from DW images to ADC maps. In the study, we chose only the largest abnormal adenopathies and excluded from analysis the necrotic areas.

2.1.2. Imaging analysis

The lymph nodes were characterized on the basis of internationally accepted standards for evaluating anatomic imaging data. First, the morphological features of each lymph node of interest were recorded such as the size (in shortest axial diameter), parenchymal homogeneity, areas of necrosis and nodal contour irregularity. The above findings could be detected in conventional T1-weighted, T2-weighted, and contrast material-enhanced T1-weighted images. SI in T1 and T2 WIs gives an idea about nodal activity as well as its contrast uptake (the malignant nodes show more contrast enhancement).

Second, the DW images and their corresponding ADC map were analyzed in consensus at a picture archiving and communication system workstation. The lymph nodes were localized on the images obtained with a *b* value of 0 s/mm^2. For quantitative assessment, regions of interest were placed in the lymph nodes identified on the *b* _ 0 images, and the software automatically copied these regions onto the other *b* value images. For the entirely solid lymph nodes, the regions of interest were placed over the entire lymph node. In cases of obvious solid and necrotic components depicted on the conventional MRI, regions of interest were placed on the solid tissue portions.

Finally, the histopathology and radiologic findings were correlated – as a reference standard – after all image interpretations had been concluded. The optimal ADC b0-1000 threshold for differentiating a benign from a malignant lymph node was determined by using receiver operating characteristic analysis. The sensitivity, specificity, and accuracy of the ADC b0-1000 were subsequently calculated.

We depend in our study on both the ADC value and signal intensity in evaluating the affected lymph node.

3. Statistical analysis

Data were statistically described in terms of mean ± standard deviation (±SD), and range, or frequencies (number of cases) and percentages when appropriate. Comparison of numerical variables between the study groups was done using Student's *t* test for independent samples. For comparing categorical data, Chi square (χ^2) test was performed. Exact test was used instead when the expected frequency is less than 5. Accuracy was represented using the terms sensitivity, and specificity. Receiver operator characteristic (ROC) analysis was used to determine the optimum cut off value for the studied diagnostic markers. *P* values less than 0.05 were considered statistically significant. *P* value >0.05 was considered insignificant.

P value <0.05 was considered significant.
P value <0.01 was considered highly significant.

All statistical calculations were done using computer programs SPSS (Statistical Package for the Social Science; SPSS Inc., Chicago, IL, USA) version 15 for Microsoft Windows.

4. Results

The pool of this study was 26 patients and the results were analyzed as follows.

4.1. Patients' characteristics

26 patients were included in this study, 9 males (35%) and 17 females (65%) (Table 1). Their age ranged from: 6–76 years, mean age 45 ± 18.8 years.

Table 1 Age and sex distribution according to histopathological diagnosis.

Case diagnosis	Gender		Age
	Male: N	Female: N	Mean (SD)
Acute lymphocytic leukemia	1	–	9
Hodgkin lymphoma	2	–	11 (7.07)
Non Hodgkin lymphoma	1	2	68 (8.08)
Metastatic differentiated carcinoma	3	6	53 (7.83)
Metastatic undifferentiated carcinoma	1	3	55 (10.8)
Acute Reactive lymphadenitis	1	–	16
Chronic granulomatous inflammation	–	1	35
Chronic non specific inflammation	–	2	31 (6.36)
Reactive lymphoid hyperplasia	–	3	44 (11)

4.2. Histopathologic diagnosis

Histopathological analysis was done dividing the examined lymph nodes in our study ($n = 32$) into 2 categories:

(A) Malignant lymphadenopathy 75% (n = 24) subdivided as follows; acute lymphocytic leukemia ($n = 2$), Hodgkin lymphoma ($n = 2$), Non Hodgkin lymphoma ($n = 4$), metastatic differentiated carcinoma ($n = 10$), metastatic undifferentiated carcinoma ($n = 6$) and *(B) benign lymphadenopathy 25% (n = 8)* subdivided into acute reactive lymphadenitis ($n = 1$), chronic granulomatous inflammation ($n = 1$), chronic non specific inflammation ($n = 2$) and reactive lymphoid hyperplasia ($n = 4$).

4.3. MRI diagnosis according to recorded ADC values

DWI and ADC values revealed 27 malignant lesions (84%), 5 benign (16%) the accuracy of the MRI was 89% in our study.

4.4. Image evaluation

1- Conventional MRI (T1 and T2 weighted images): for size and parenchymal architecture evaluation of the lymph nodes.
- Size criteria among the benign and malignant LNs (in shortest axis diameter).

The size of the examined lymph nodes ($n = 32$) ranged from 0.6 to 2.5 cm (mean size 1.2 ± 0.44 cm).

23 nodes were 1 cm or more in diameter; 17 malignant and 6 benign LNs while 9 nodes were less than 1 cm in diameter; 7 malignant and 2 benign LNs. Ratio between the longest and shortest axial diameter was 1.5:1.

4.5. Parenchymal architecture among the benign and malignant LNs

Among the malignant lymphadenopathy group ($n = 24$), 19 nodes exhibited homogenous solid architecture (79.2%) and 5 nodes exhibited heterogeneous architecture of the parenchyma (20%). Among the benign lymphadenopathy group ($n = 8$), all nodes exhibited homogenous solid architecture of the parenchyma (100%). These changes in nodal architecture were well depicted on T2-weighted images.

2- Diffusion WIs

All malignant nodes ($n = 24$) show restricted diffusion evidenced by increased signal on increasing the b-values ($b = 1000$) and low signal on ADC maps. In 5/8 cases with inflammatory diseases, lymph nodes showed reduction of signal intensity on increasing b values ($b = 1000$) and intermediate signal intensity on ADC maps reflecting facilitated diffusion. 3/8 cases of benign lymphadenopathy, diagnosed as reactive lymphoid hyperplasia and chronic granulomatous infection show increased signal on increasing b-values (false positive).

3- ADC values among the malignant and benign LNs

- ADC values were obtained and recorded for all 32 cervical lymph nodes detected at consensus reading.

(A) Malignant lymph node group

ADC values of the malignant lymph ($n = 24$) ranged between 0.567 and 0.98×10^{-3} mm^2/s (Table 2). The mean ADC value of malignant lymph nodes was $0.774 \pm 0.11 \times 10^{-3}$ mm^2/s.

Among the subgroups of malignant lymph nodes: The mean ADC value of metastatic differentiated carcinoma (0.83×10^{-3} mm^2/s) was slightly higher (i.e., less restricted) than the mean ADC values of undifferentiated carcinoma (0.811×10^{-3} mm^2/s), Hodgkin lymphoma (0.734×10^{-3} mm^2/s) and non Hodgkin lymphoma (0.686×10^{-3} mm^2/s) in the descending order. There were no statistically significant differences in ADC values among the different subgroups of malignant lymph nodes.

The patient with Hodgkin disease who received chemotherapy, had undergone follow up DW MRI, lymph nodes were hypointense on DWI ($b = 1000$) and intermediate signal on the ADC maps with a mean ADC value of 1.2×10^{-3} mm^2/s (compared to ADC 0.687×10^{-3} mm^2/s pretreatment) indicating facilitated diffusion.

Table 2 Comparison of ADC values among benign and malignant LN groups.

ADC value			
	Range	Mean	SD
Malignant	0.567–0.98	0.774	0.11
Benign	0.712–1.3	1.019	0.20

(B) Benign lymph node group

ADC values of benign lesions ranged between 0.712×10^{-3} and 1.3×10^{-3} mm^2/s (Table 2). The mean ADC value of the benign lymph nodes ($n = 8$) was $1.019 \pm 0.20 \times 10^{-3}$ mm^2/s. The highest mean ADC value was for acute lymphadenitis. Among the benign lesions, chronic granulomatous inflammation ($n = 1$) and reactive lymphoid hyperplasia ($n = 3$) had low ADC values similar to the malignant group.

The mean ADC value of malignant nodes was lower than the mean ADC value of benign nodes. The difference between the mean ADC values of benign and malignant lesions was statistically significant ($P < 0.0001$).

A threshold ADC value for differentiating malignant from benign nodes derived with receiver operating characteristic analysis equals 1.005×10^{-3} mm^2/s (Fig. 1).

The statistical data obtained were 24 true-positive, 3 false-positive, 5 true-negative findings, yielding 100% sensitivity, 62.5% specificity%, NPV = 100% and PPV = 89% (Table 3).

Table 3 ADC–pathology correlation.

	Frequency	Percentage (%)
True positive	24	75
False positive	3	9.4
True negative	5	15.6
Total	32	100

5. Discussion

Diffusion weighted imaging (DWI), a well-known MRI-technique in neuroradiology, has shown its potential to be a reliable non-invasive imaging technique for tissue characterization. DWI exploits the random motion of water in the targeted tissue, which reflects the tissue specific diffusion capacity. Thus, the diffusion capacity can be used for tissue characterization. In biologic tissues, the diffusivity of water molecules is confined by the intra-cellular and inter-cellular spaces. Hyper cellular tissue, such as malignant tumors, results in decreased mobility of water protons and consequently in a restricted diffusion capacity of the tissue. Thus, tumors present with increased signals on DWI and low ADC values. Non-tumoral tissues such as edema, inflammation, fibrosis, and necrosis are expected to show low cellularity–in strong contrast with viable tumor. In these tissues the diffusion capacity is not restricted. This results consecutively in a signal loss on DWI and in a high ADC (6). The evaluation of cervical adenopathies is important as they serve as an excellent clue to underlying problems. They could be due to infections, autoimmune disorders or malignancies (metastatic or lymphomas) (1).

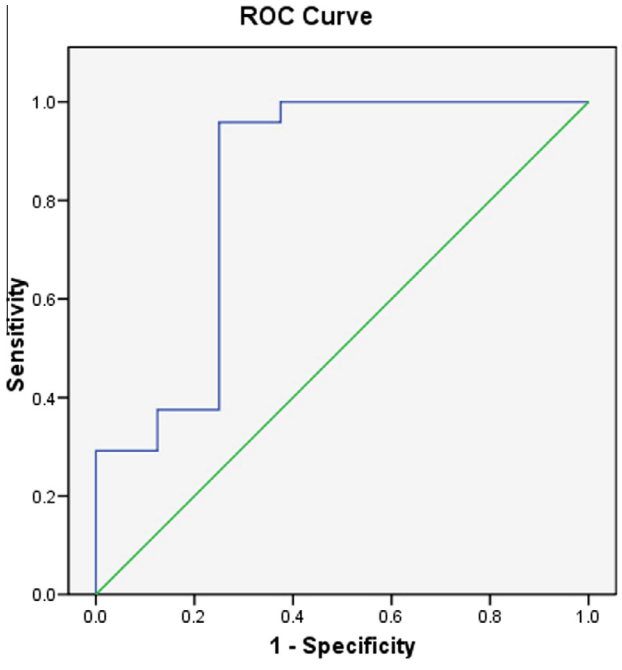

Figure 1 Receiver operating characteristic (ROC) curve of the ADC values used for differentiating benign from malignant lymph nodes. The area under the curve of 0.828. We obtained the threshold ADC value for differentiating benign from malignant nodes from this ROC curve = 1.005×10^{-3} mm^2/s.

Ultrasound image, contrast-enhanced computed tomographic and contrast-enhanced MRI allow the detection of enlarged cervical lymphadenopathies. None of these methods reaches the ideal accuracy in diagnosis (14). These imaging methods use standard parameters (shape, size, internal architecture, extranodal diffusion and vascular features). The size is the most used criterion for the diagnosis (3). The criterion of a short-axis diameter of 10 mm has gained widespread acceptance (2) and thus used in our study. To date, the diagnosis of lymph node metastases is based mainly on size criteria; however, non enlarged nodes may harbor malignancy, whereas reactive nodes may be enlarged. Promising results with DW imaging to help detect cervical lymph node metastases and differentiate between benign and malignant enlarged nodes have been reported by (5). Other criteria have proven to be unreliable as internal necrosis because they may also be detected in non-metastatic disease including inflammation, infection and autoimmune disease (6).

SPECT (single photon emission CT) and PET (photon emission tomography) are new imaging techniques which supply functional information (blood flow and glucidic metabolism) but they are invasive (exposure to radiations), expensive, not easily available and with a relatively low spatial resolution (15).

First results were obtained by (7) from lymph nodes of the head and neck region using a navigated DW-EPI with a b factor of 0 s/mm^2 and 800 s/mm^2. Regular (benign) lymph nodes showed significantly higher diffusivity than that of metastatic lymph nodes.

Our study had been conducted on 26 patients, mean age was 45 ± 18.8 years. The prevalence of Hodgkin disease ($n = 2$) and leukemia ($n = 1$) was higher in young age groups; mean age in HD and leukemic patients was 11 and 9 years respectively while the prevalence of non Hodgkin disease ($n = 3$) was higher among the elderly age group; mean age was 68 years. Otherwise, there is no significant difference according to age or gender of patients.

In this study, DW imaging with the use of ADCb0-1000 values had high accuracy in the detection of metastatic lymph nodes, mainly by improving the detection of subcentimeter

nodal metastases. Our study included 9 nodes less than 1 cm in its shortest axis diameter; 7/9 were metastatic – and showed restricted pattern on DWIs and corresponding low ADC value – on the other hand, these 9 nodes show no distinctive morphologic features of malignancy, such as necrosis and indistinct margins in conventional MRI and differentiation of metastatic nodes would have been quite impossible. These results were in line with other studies, (2) stated that nearly all metastatic lymph nodes smaller than 1 cm were missed owing to the size-based criteria for anatomic MR imaging. Therefore, it has been concluded that DW imaging could provide additional value to an anatomic MR examination, especially in subcentimeter-sized lymph nodes. Several factors enable the detection of small nodal metastases at DW imaging. Use of improved echo-planar imaging technology, dedicated coils, and dedicated sequence optimization enables a maximal reduction of echo-planar imaging-related artifacts at a relatively high spatial resolution.

De Bondt et al., (16) also concluded that with predominantly small lymph nodes, the ADC criterion is the strongest independent predictor of the presence of metastasis. The use of ADC values in combination with the other MRI criteria significantly improves the discrimination between malignant and benign lymph nodes with a sensitivity and specificity 92.3% and 83.9% respectively.

In our study, 3/10 metastatic differentiated squamous cell carcinomas lymph nodes (< 1 cm) were detected on the contralateral side to the primary tumor (postcricoid, lip SCC) whereas 1/10 node (1 cm) detected on the contralateral side of the primary tumor (retromolar cancer) had proven benign. These findings had been stated in the literature, (8) reported the degree to which DW imaging changes the accuracy of nodal differentiation, by depicting subcentimeter nodal metastases which may affect the clinical management in specific situations. In cases of head and neck tumors growing close to the midline or extensive ipsilateral nodal metastatic involvement, the detection or exclusion of metastatic spread to the contralateral neck is pivotal to treatment. As such, the technique has potential value as an ancillary tool for not only determining the extent of neck dissection required for advanced stage disease but also planning radiation therapy.

Use of this technique also improved the identification of benign enlarged lymph nodes. Our study included 23 nodes of 1 cm or more in shortest axial diameter; and 6/23 were benign inflammatory LNs with non restricted pattern.

This study was conducted with high b value (b = 1000 s/mm^2) to overcome the effect of capillary perfusion and water diffusion in extracellular extravascular space, as high b value will result in the reduction of signal from moving protons in vessels. Using higher b-values, thus, will improve the specificity of the contrast on DWI. Furthermore, the differences in the relative contrast ratio between malignant and benign lesions were increased with a high b value. This was similar to the b values used in studies carried out by (2,9,3).

In our study, all malignant nodes (n = 24) show restricted diffusion evidenced by increased signal on increasing the b-values (b = 1000) and low signal on ADC maps. 5/8 cases with inflammatory diseases, lymph nodes showed reduction of signal intensity on increasing b values and intermediate signal intensity on ADC maps reflecting facilitated diffusion (b = 1000). These data are similar to those in the literature, (3,2) reported that metastatic and lymphomatous nodes present a reduction of diffusivity, which can be attributed to a hypercellularity, cellular pleomorphism, increased mitosis and nuclear-to-cytoplasmatic ratio. These features probably diminish the extracellular extravascular space.

These results are in line with (17) who concluded that DWI-MRI performed with ADC values shows significant differences among malignant nodes, lymphomatous nodes, and benign nodes in cervical lymphadenopathy.

In our study, the difference between the mean ADC values of benign and malignant lesions was statistically significant (P < 0.0001) which was in line with (2) which reported that the mean ADC value derived from the signal intensity across images (ADC b0-1000) of benign lymph nodes was higher than that of malignant LNs and these differences were statistically significant (P < 0.0001). Perronea (3) reported that ADC values of benign lymph nodes were significantly higher than those of malignant LNs, with a P value < 0.01 and the mean ADC value for malignant lesions, that was 0.85×10^{-3} mm^2/s, which is lower than that of benign LNs, that was 1.448×10^{-3} mm^2/s. The best ADC threshold value for distinguishing benign from malignant nodes was 1.03×10^{-3} mm^2/s, with a sensitivity of 100% and a specificity of 92.9%.

The best threshold for differentiating malignant from benign lymph nodes was 1.15×10^{-3} mm^2/s (18).

Holzapfel et al. (9) reported an accuracy of 94% in characterizing metastatic lymph nodes when using a threshold of 1.02×10^{-3} mm^2/s. Their reported mean ADC values for benign and metastatic lymph nodes were $1.24 \pm 0.16 \times 10^{-3}$ mm^2/s and $0.78 \pm 0.09 \times 10^{-3}$ mm^2/s, respectively.

In our study, the mean ADC value of the 24 malignant lymph nodes was $0.774 \pm 0.11 \times 10^{-3}$ mm^2/s whereas the mean ADC value of the 8 benign lymph nodes was $1.019 \pm 0.20 \times 10^{-3}$ mm^2/s with a threshold ADC value for differentiating malignant from benign nodes derived with receiver operating characteristic analysis of 1.005×10^{-3} mm^2/s with a sensitivity of 100% and a specificity of 62.5%.

In our study, one patient with Hodgkin disease who received chemotherapy, had undergone follow up DW MRI, lymph nodes were hypointense on DWI (b = 1000) and intermediate signal on the ADC maps with a mean value of 1.2×10^{-3} mm^2/s (compared to ADC 0.687×10^{-3} mm^2/s pretreatment) indicating facilitated diffusion. This finding was in line with previous studies.

Thoeny et al. (5) reported that after chemotherapy or radiation therapy, residual changes or even masses are commonly observed at the primary or nodal site, and conventional morphologic MR imaging currently encounters difficulty in helping distinguish between benign post treatment alterations and residual cancer.

Studies done by (10) showed that the ADC of residual or recurrent squamous cell carcinoma is significantly lower than that of a post treatment non tumoral residual mass, and similar ADC thresholds of around 1.3 mm^2/s have been identified in these studies.

In our study, malignant lymph nodes were subdivided according to histopathology into subgroups: metastatic differentiated carcinoma, metastatic undifferentiated carcinoma, Hodgkin and non Hodgkin lymphoma. An attempt to differentiate between them on basis of their ADC values was made. The mean ADC value of metastatic differentiated carcinoma (0.83×10^{-3} mm^2/s) was slightly higher (i.e., less restricted) than the ADC value of undifferentiated carcinoma

(0.811×10^{-3} mm^2/s), Hodgkin lymphoma (0.734×10^{-3} mm^2/s) and non Hodgkin lymphoma (0.686×10^{-3} mm^2/s) in the descending order. There were no statistically significant differences in ADC values among the different subgroups of malignant lymph nodes.

Regarding the former mentioned issue, statistically significant results were reported in the literature. King et al., (11) reported that Diffusion-weighted MR imaging shows significant differences among malignant nodes of differentiated carcinoma, lymphoma, and undifferentiated carcinoma.

In our study, the statistical data obtained were 24 true-positive, 3 false-positive, 5 true-negative findings, yielding 100% sensitivity, 62.5% specificity%, NPV = 100% and PPV = 89%.

The false positive results were previously described by (12), in benign lymph nodes, a false decrease in ADC may correlate with the presence of nodal reactive changes that manifest as multiple germinal centers and fibrotic stroma, which act as microstructural barriers. Vandecaveye et al, (2) as well described a false decrease in ADC due to nodal reactive changes which may lead to an overestimation of the metastatic burden. In their study, this was reflected by the lower specificity of DW imaging, as compared with conventional MR imaging, in the detection of subcentimeter nodal metastases. The combined use of DW imaging and anatomic features indicative of benignity may help to decrease the false-positive rate.

Choi et al. (13) stated that other false-positive readings may be due to restricted diffusion in recent hemorrhage or hematoma. Therefore, DW imaging probably should not be performed directly after biopsy.

5.1. Our study had some limitations

First, our study has some limits such as being a small study cohort.

Second, we did not report normalized ADCs for several reasons: the benefit of using normalized rather than absolute ADCs at DW imaging of the head and neck has never been reported. In contrast to the brain, the head and neck area is characterized by highly heterogeneous tissue diffusivity owing to the presence of tissues of a distinctly different histologic origin. Therefore, the spine is probably the most suitable reference tissue for normalization purposes. However, spinal cord echo-planar imaging is hindered by strong susceptibility influences—induced mainly by the surrounding osseous elements of the spinal column—that introduce additional variability in ADC calculations also the promising results of the current study, which were achieved by using absolute ADCs, might indicate that normalization is not mandatory, facilitating the implementation of DW imaging into routine clinical practice.

6. Conclusion

MR diffusion imaging could be an important supportive tool in differentiation between benign and malignant lymph nodes, can to a lesser extent differentiate between the types of malignant lymphadenopathy and can be used as an indicator for treatment response post chemo and radiotherapy and detection of residual/recurrent pathology.

Case 1: A 6 year old male patient presenting with left sided progressive neck swelling (Fig. 2).

MR findings: Multiple enlarged left deep cervical lymph nodes: level IV and V of lobulated smooth contours.

Size: The largest measures 2.5 cm in its shortest transverse diameter.

Parenchymal architecture: They show low homogenous T1 signal changing into intermediate/high T2 signal with faint heterogenous contrast uptake.

On DWIs: In DWIs: b0 and b1000, they are partially hyperintense corresponding to lymph nodes of low signal in ADC map (restricted pattern).

ADC values: were recorded as follows	
Group IV	0.825×10^{-3} mm^2/s
Group V	0.787×10^{-3} mm^2/s

Suggested MR diagnosis: Malignant lymphadenopathy.

Biopsy results: Hodgkin lymphoma (nodular lymphocytic dominance).

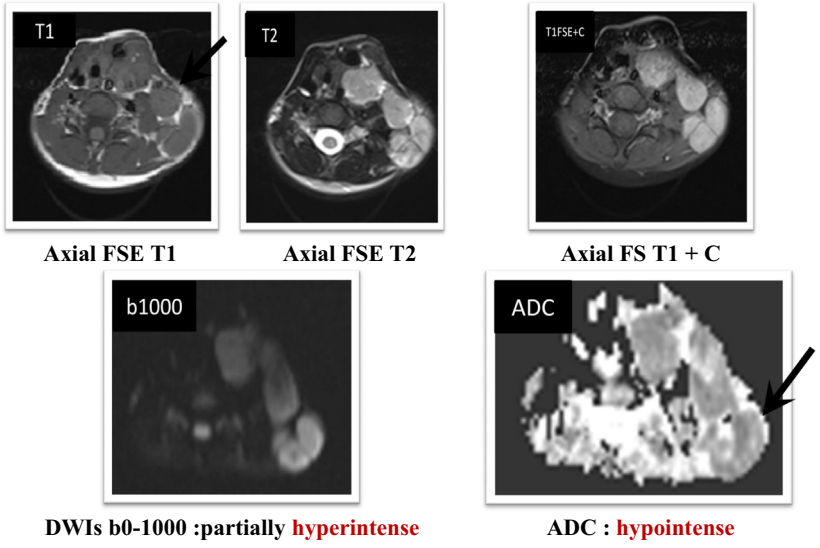

Figure 2 A 6 year old male patient presenting with left sided progressive neck swelling.

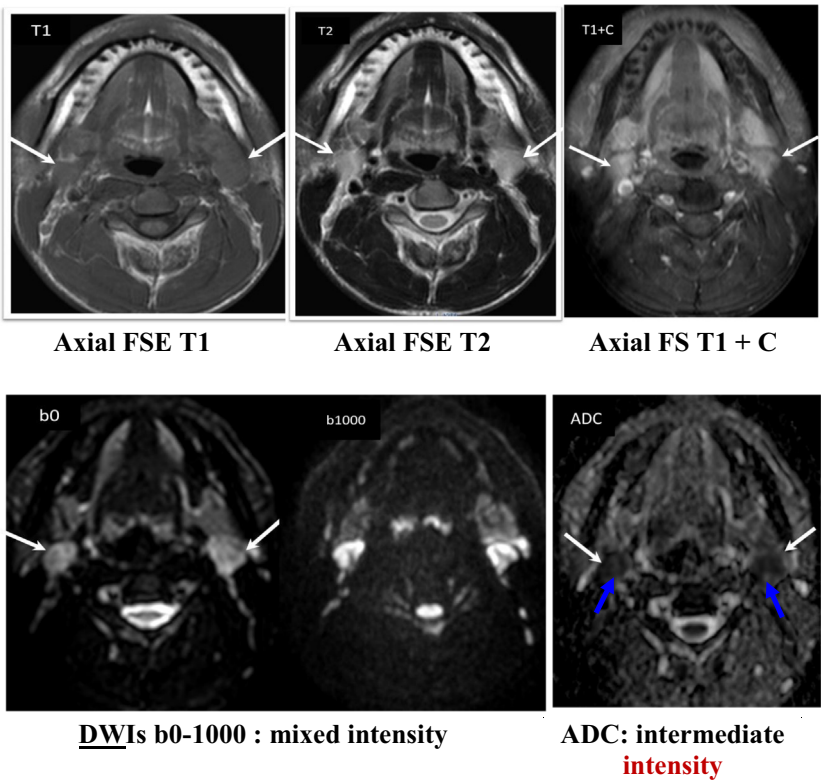

Figure 3 A 16 year old male patient presenting with bilateral neck swellings of acute onset, regressive course on antibiotics.

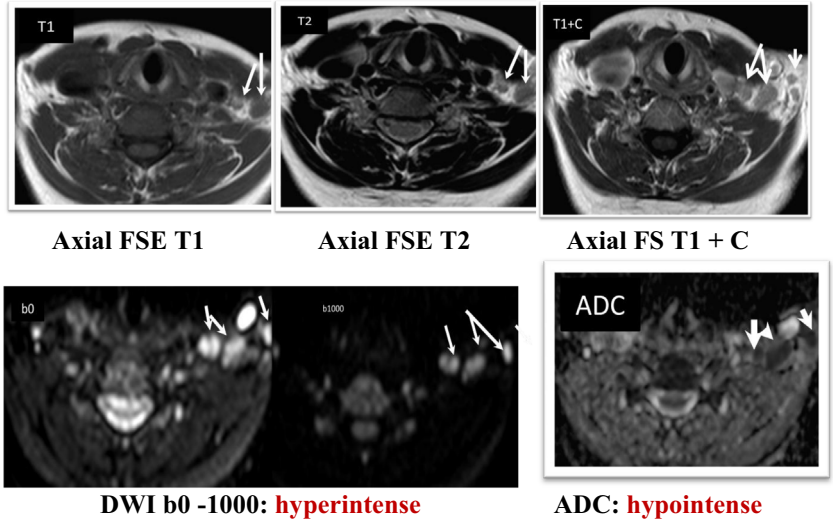

Figure 4a Left metastatic undifferentiated carcinoma.

Follow up diffusion imaging post chemotherapy: ADC value of residual lymph nodes was 1.16×10^{-3} mm^2/s (facilitated pattern) indicating good therapeutic response.

Case 2: A 16 year old male patient presenting with bilateral neck swellings of acute onset, regressive course on antibiotics (Fig. 3).

MR findings: Bilateral enlarged upper deep cervical lymph node level IIa showing smooth contours. The largest on the left side measures 1.3 cm in its shortest transverse diameter. They exhibit isointense T1 signal changing into high T2 signal with fair homogenous contrast uptake.

On DWIs: In DWIs: b0 and b1000, they are partially hyperintense corresponding to lymph nodes of intermediate mixed signal in ADC map.

ADC value: 1.3×10^{-3} mm^2/s. ROI was in the central relatively hyper intense area of the node (blue arrows in ADC image).

Suggested MR diagnosis: morphologically and by ADC value appear to be benign lymphadenopathy.

Biopsy results: Reactive lymphadenitis.

Case 3: A 49 year old female patient presenting with left neck swellings of insidious onset. No known primary. Neck

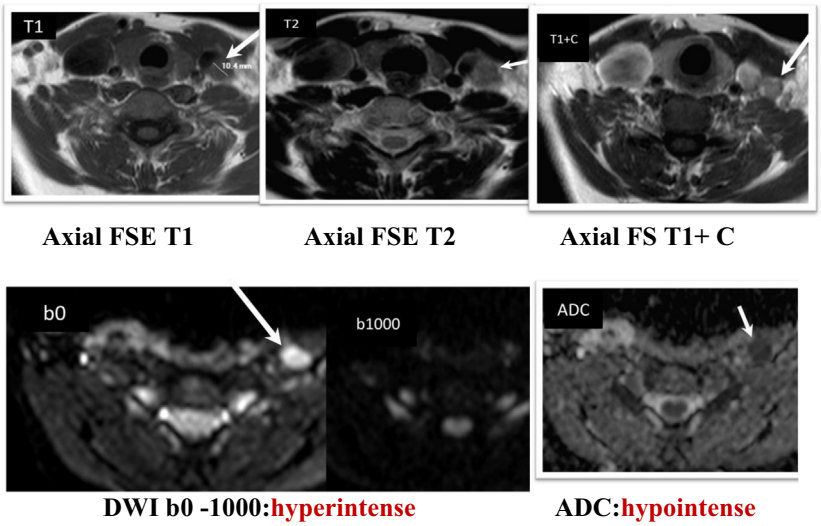

Figure 4b Left metastatic undifferentiated carcinoma (lower cuts).

US was done revealing enlarged left lower cervical lymph nodes (Figs. 4a and b).

MR findings: Left enlarged lower deep cervical lymph nodes: level IV and V lymph nodes with regular contour (Fig. 4a).

Size: Shortest transverse diameter of 0.6 cm and 1 cm respectively.

Parenchymal architecture: They exhibit isointense homogenous T1 and intermediate T2 signals with faint contrast uptake in post contrast series. Lower level left level IV lymph node with partially ill defined margins (Fig. 4b).

Size: shortest transverse diameter of 1.04 cm.

Parenchymal architecture: It exhibits isointense homogenous T1 and intermediate T2 signals with faint contrast uptake in post contrast series.

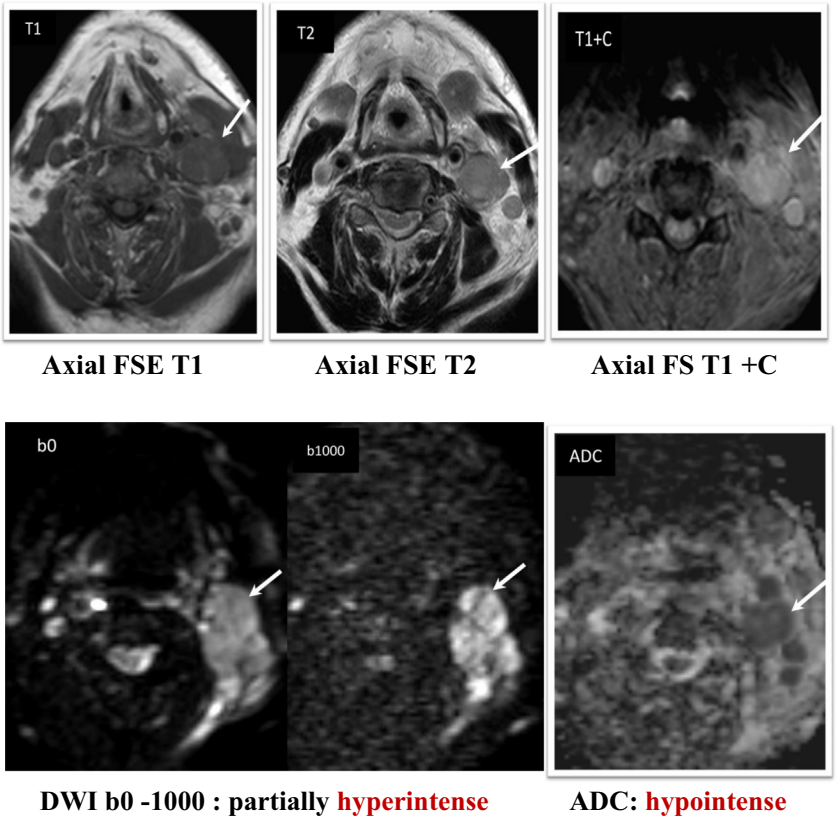

Figure 5 A 76 year old male patient presenting with left sided neck swellings of insidious onset. No known primary.

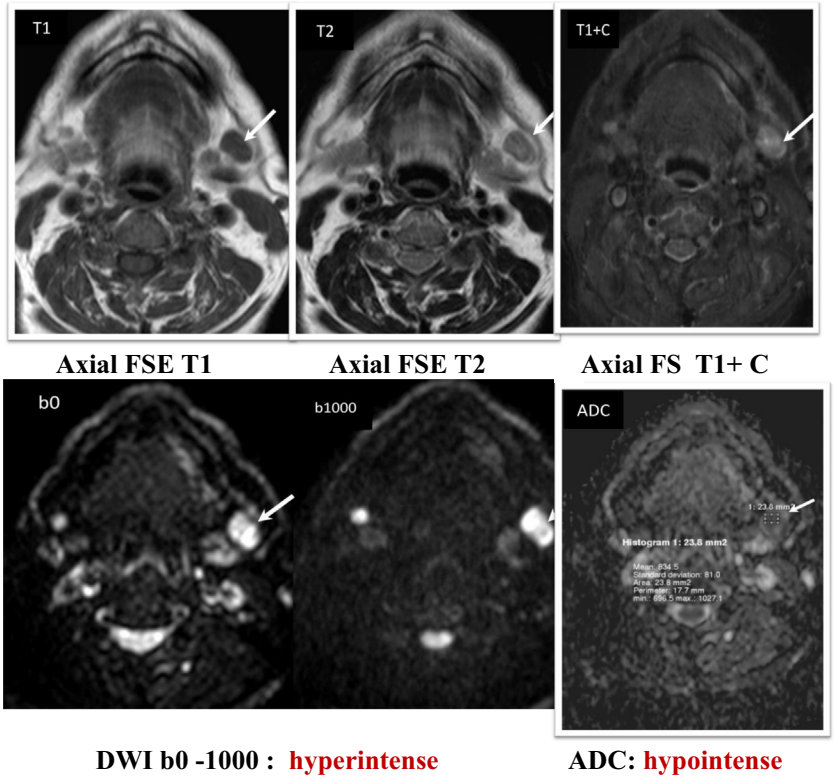

Figure 6 A 55 year old male presenting with left sided retromolar malignant mass of insidious onset. MRI neck was done for staging.

On DWIs: In DWIs: b0 and b1000, all lymph nodes are hyperintense corresponding to lymph nodes of low signal in transverse ADC map. (Restricted pattern).

ADC value: (a) 0.947×10^{-3} mm^2/s (group IV) and 0.825×10^{-3} mm^2/s (group V), (b) 0.838×10^{-3} mm^2/s (group IV).

Suggested MR diagnosis: Malignant lymphadenopathy.

Biopsy results: Metastatic undifferentiated carcinoma, grade 3 (Initial presentation).

Case 4: A 76 year old male patient presenting with left sided neck swellings of insidious onset. No known primary (Fig. 5).

MR findings: Enlarged left upper and lower deep cervical lymph nodes: largest in level III showing lobulated smooth contours.

Size: 2.3 cm in its shortest transverse diameter.

Parenchymal architecture: They show isointense T1 signal changing into high T2 signal with faint homogenous contrast uptake.

On DWIs: In DWIs: b0 and b1000, they are partially hyperintense corresponding to lymph nodes of low signal in ADC map.

ADC value: 0.57×10^{-3} mm^2/s.

Suggested MR diagnosis: Malignant lymphadenopathy.

Biopsy results: Non Hodgkin lymphoma.

Case 5: A 55 year old male presenting with left sided retromolar malignant mass of insidious onset. MRI neck was done for staging (Fig. 6).

MR findings: Left upper deep cervical lymph node level Ib showing smooth contour.

Size: 0.7 cm in its shortest transverse diameter.

Parenchymal architecture: It shows isointense T1 signal changing into high T2 signal with fair homogenous contrast uptake.

On DWIs: In DWIs: b0 and b1000, it shows hyperintense signal corresponding to lymph node of low signal in ADC map.

ADC value: 0. 834×10^{-3} mm^2/s.

Suggested MR diagnosis: Malignant lymphadenopathy.

Biopsy results: Metastatic SCC.

Conflict of interest

Evaluation of the role of diffusion weighted MRI in the evaluation of cervical lymphadenopathy trying to differentiate benign from malignant nodes.

References

(1) Sambandan T, Christefi Mapel R. Review of cervical lymphadenopathy. JIADS 2011;2(1):31–3.
(2) Vandecaveye V, De Keyzer F, Vander Poorten V, et al. Head and neck squamous cell carcinoma: value of diffusion-weighted MR imaging for nodal staging. Radiology 2009;251(1):134–46.
(3) Perronea A, Guerrisia Pietro, Izzob Luciano, et al. Diffusion-weighted MRI in cervical lymph nodes: differentiation between benign and malignant lesions. Eur J Radiol 2011;77:281–6.
(4) Abdel Razek AA, Soliman NY, Elkhamary S, et al. Role of diffusion-weighted MR imaging in cervical lymphadenopathy. Eur Radiol 2006;16:1468–77.

(5) Theony Harriet C, Keyzer Frederik De, King Ann D. Diffusion weighted MR imaging of head and neck. Radiology 2012;263(1):9–32.
(6) Herneth AM, Mayerhoefer M, Schernthaner R, et al. Diffusion weighted imaging: lymph nodes. Eur J Radiol 2010;76:398–406.
(7) Herneth AM, Czerny C, Krestan C, et al. Role of diffusion weighted MRI in the characterization of lymph node metastasis. XVI International Congress of Head and Neck Radiology (ICHNR) 2003;238(2):604–10.
(8) MWM Van den Brekel, Castelijns J A. What the clinician wants to know: surgical perspective and lymph node imaging of the neck. Cancer Imaging 2005;5:41–9 (spec no A).
(9) Holzapfel K, Duetsch S, Fauser C, et al. Value of diffusion-weighted MR imaging in the differentiation between benign and malignant cervical lymph nodes. Eur J Radiol 2009;72(3):381–7.
(10) Abdel Razek AA, Kandeel AY, Soliman N, et al. Role of diffusion-weighted echo-planar MR imaging in differentiation of residual or recurrent head and neck tumors and posttreatment changes. AJNR Am J Neuroradiol 2007;28(6):1146–52.
(11) King AD, Ahuja AT, Yeung DK, et al. Malignant cervical lymphadenopathy: diagnostic accuracy of diffusion-weighted MR imaging. Radiology 2007;245:806–13.
(12) Wang J, Takashima S, Kawakami F, et al. Head and neck lesions: characterization with diffusion-weighted echo-planar MR imaging. Radiology 2001;220:621–30.
(13) Choi KD, Jo JW, Park KP, et al. Diffusion weighted imaging of intramural hematoma in vertebral artery dissection. J Neurol Sci 2007;253:81–4.
(14) Esen G. Ultrasound of superficial lymph nodes. Eur J Radiol 2006;58:345–59.
(15) Yamazaki Y, Saitoh M, NotaniK, et al. Assessment of cervical lymph node metastases using FDG-PET in patients with head and neck cancer. Am Nucl Med 2008;22:177–84.
(16) De Bondt RB, Hoberigs MC, Nelemans PJ. Diagnostic accuracy and additional value of diffusion-weighted imaging for discrimination of malignant cervical lymph nodes in head and neck squamous cell carcinoma. Neuroradiology 2009;51:183–92.
(17) Wu LM, Xu JR, Hua J. Value of diffusion-weighted MR imaging performed with quantitative apparent diffusion coefficient values for cervical lymphadenopathy. J Magn Reson Imaging 2013;38(3):663–70.
(18) Tamer F, Ali Taha. Neck lymph nodes: characterization with diffusion-weighted MRI. Egypt J Radiol Nucl Med 2012;43(2):173–81.